Journal of Alloys and Compounds 671 (2016) 545–551

Contents lists available at ScienceDirect

Journal of Alloys and Compounds

journal homepage: http://www.elsevier.com/locate/jalcom

Low-temperature structural and magnetic phase transitions in multiferroic $GdFe_3(BO_3)_4$

K.V. Frolov [a, *], I.S. Lyubutin [a], E.S. Smirnova [a], O.A. Alekseeva [a], I.A. Verin [a], V.V. Artemov [a], S.A. Kharlamova [b], L.N. Bezmaternykh [c], I.A. Gudim [c]

[a] Shubnikov Institute of Crystallography, Russian Academy of Sciences, 119333, Moscow, Russia
[b] Geophysical Laboratory, Carnegie Institution of Washington, Washington DC 20015, USA
[c] Kirensky Institute of Physics, Siberian Branch of Russian Academy of Sciences, 660036, Krasnoyarsk, Russia

ARTICLE INFO

Article history:
Received 17 November 2015
Received in revised form
7 February 2016
Accepted 9 February 2016
Available online 15 February 2016

Keywords:
Multiferroics
Rare earth compounds
X-ray diffraction
Mössbauer spectroscopy
Crystal structure
Spin dynamics

ABSTRACT

X-ray analysis revealed that at temperature decreasing from room temperature to $T_{str} = 155$ K the crystal unit cell $GdFe_3(BO_3)_4$ is reduced only along the *c* axis (at 0.01 Å), while the *a* and *b* axes are unchanged within the error limits. The volume of the crystal decreases uniformly in the direction of all three axes at 155–80 K. At 80–30 K the crystal volume is decreased only by reduction of the parameters *a* and *b*, while the parameter *c* increases conversely. In the paramagnetic region Mössbauer spectra do not distinguish between the two structural positions of iron ions Fe1 and Fe2, appearing at $T < T_{str}$. Below the temperature of the magnetic phase transition at $T_N = 38.0(1)$ K the Mössbauer data indicate quasi-one-dimensional magnetic ordering of iron moments in the sublattice Fe2 and a two-dimensional one in the iron sublattice Fe1. The dynamics of spin reorientation in sublattices Fe1 and Fe2 is studied in detail.

1. Introduction

Recently, the study of multiferroic materials has raised considerable interest due to their large magnetoelectric effect [1–7]. Among such materials there is a new family of rare earth borates $RM_3(BO_3)_4$ (R = rare earth element, M = Al, Ga, Fe, Sc). The crystals of this family are isostructural to the natural mineral huntite, $CaMg_3(CO_3)_4$ [8], and have trigonal symmetry with space group $R32$ (D^7_{3h}) [9,10]. The rare earth aluminum-borates show nonlinear optical and laser properties. For example, $YAl_3(BO_3)_4$ and $GdAl_3(BO_3)_4$, doped with neodymium, may be used for the frequency-doubled lasers. $GdAl_3(BO_3)_4$:Nd^{3+} crystal is one of the most effective materials for diode pump lasers with self-doubling frequency, while $NdAl_3(BO_3)_4$ is an effective medium for mini-lasers [11–13]. The compounds with magnetic ions M = Cr, Fe can be used in magneto-optical devices based on the Kerr and Faraday effects. Magnetoelectric interactions in rare-earth ferroborates appear as anomalies in the dependence of the electric polarization on the magnetic field when the magnetic structure in the iron sublattice changes [14–16]. The presence of two magnetic subsystems, iron ions and rare earth ions, generates a diversity of the ferroborates properties [16].

One of the most interesting compounds in the family is $GdFe_3(BO_3)_4$ because it shows the cascade of phase transitions discovered in the past two decades. Its magnetic susceptibility, magnetization, and heat capacity measurements [17–19] have shown that at low temperatures $GdFe_3(BO_3)_4$ is a compensated antiferromagnet with the Neel temperature $T_N = 38$ K and the spin reorientation transition happens in the crystal at about $T_{SR} = 10$ K (spin flop). Below T_N the magnetic ordering refers to iron ions, however when the temperature is lowered further the paramagnetic Gd^{3+} ions are magnetized by iron sublattice and affect the anisotropic properties of the crystal significantly [20–23]. X-ray diffraction and Raman studies as well as the data on heat capacity have shown a structural phase transition at about $T_{str} = 155$ K [19,26,27]. When applying high pressure to $GdFe_3(BO_3)_4$ crystal, the structural phase transitions and two electronic transitions with an abrupt decrease in the optical gap to a value characterizing a semiconducting state have been discovered at pressures of $P = 26$ and 43 GPa [24,25]. The observation of magnetoelectric effects [6] has allowed to assign $GdFe_3(BO_3)_4$ to the multiferroic category of

* Corresponding author.
E-mail address: green@crys.ras.ru (K.V. Frolov).

http://dx.doi.org/10.1016/j.jallcom.2016.02.083
0925-8388/

materials. It is recently established [23] that electric polarization is induced by both magnetic subsystems of Fe and Gd ions. The contribution from iron ions is isotropic, and from gadolinium ones is anisotropic.

Despite the large number of publications, the feature of the magnetic ordering of iron and gadolinium ions, and the relationship between the structural and magnetic phase transitions in $GdFe_3(BO_3)_4$ remain unclear. Low-temperature structural studies were conducted only at 90 K [26], which is not sufficient for complete understanding of the properties of this crystal. In this paper, the dynamics of structural and magnetic phase transitions in $GdFe_3(BO_3)_4$ single crystal was investigated by X-ray diffraction at the temperature range 30–295 K and by Mössbauer spectroscopy (on nuclei ^{57}Fe) in the range of 5–295 K.

2. Experiment

High-quality single crystals of dark green transparent $GdFe_3(BO_3)_4$ were grown by the solution of the melt (the flux method) [28,29]. Elemental chemical composition of the samples was determined by energy dispersive X-ray microanalysis using scanning electron microscope FEI Quanta 200 3D Dual Beam, equipped with a microanalyzer EDAX. The measurements at the accelerating voltage of 5 kV and 30 kV have been conducted. At 5 kV we did not succeed to achieve the necessary spatial resolution for detection of boron atoms in the structure. The measurements at 30 kV have shown that the sample contains the atoms of bismuth, Bi, in a weight amount of about 1.5%. It may be incorporated into the crystal from the solution (melt) during the synthesis, presumably substituting the gadolinium, Gd.

X-ray diffraction investigations of $GdFe_3(BO_3)_4$ single crystals were performed at the temperature range 30–295 K using 4-Circle Diffractometer HUBER-5042, equipped with a cryostat DISPLEX DE-202. In the temperature range of 20–250 K the closed-cycle cryostat provides the sample temperature stability at a level of ±0.05 K. The accuracy of setting the goniometer angular positions is 0.001°. The unit cell parameters were measured at room temperature and then in increments of 5–10 K in the temperature range 220–30 K. Structural parameters were determined from 32 reflections within a diffraction angle range of $19 < \theta < 22°$. We measured 4 axial reflections (at $2\theta = 45°$) and 12 reflections (at $2\theta = 38°$) in the positive and negative regions.

The Mössbauer measurements were performed on powdered single crystals of $GdFe_3(BO_3)_4$. Mössbauer absorption spectra at ^{57}Fe nuclei were recorded in the temperature range of 5 – 295 K using a standard spectrometer MS-1104Em operating in the constant acceleration mode and equipped with a special closed-cycle helium cryostat RTI CryoFree-104. The source of gamma rays ^{57}Co (Rh) was at room temperature. The values of the isomer shifts were measured relative to a standard absorber, α-Fe at room temperature. Computer analysis of the spectra was performed using the program Univem MS that is a part of the software of the spectrometer MS-1104Em.

3. Results and discussion

3.1. X-ray research data

The crystal structure of $GdFe_3(BO_3)_4$ (space group $R32$ at 295 K) can be represented as layers perpendicular to the c axis (C_3) and consisting of trigonal prisms, GdO_6, and smaller FeO_6 octahedra [9,10]. Boron atoms form two types of triangles [BO_3] with oxygen atoms. The vertices of the first type triangles [BO_3]1 are connected with the FeO_6 octahedra only. In the triangle of the second type [BO_3]2 the vertex is connected to two FeO_6 octahedra, and each of the other two vertices is connected to both FeO_6 octahedron and GdO_6 prism. FeO_6 octahedra are connected by edges, forming helical chains elongated along the c axis (see Fig. 1).

X-ray diffraction data in Ref. [26] were obtained for a crystal $GdFe_3(BO_3)_4$ at two temperatures 295 and 90 K. It was shown that at 295 K, all the iron ions are structurally equivalent and FeO_6 octahedra form identical helical chains along the c axis. At 90 K the crystal symmetry is reduced from $R32$ to $P3_121$ (as a consequence of the structural transition at $T_{str} = 155$ K), and the spatial position of the boron group BO_3 linking together chains of iron changes. According to the authors of [26], this leads to two non-equivalent positions of iron found at 90 K.

The results of our X-ray studies in the temperature range of 30–295 K are shown in Fig. 2. We establish here that at temperature decreasing the unit cell parameters a and b preserve their values until the temperature reaches $T_{str} = 155$ K and, then the values are reduced abruptly by 0.005 Å indicating the structural transition (see Fig. 2(a)). The parameter c behaves differently (see Fig. 2(b)). In the range of 295–160 K it reducing from 7.577(5) to 7.567(4) Å, then it experience a little sharp drop at 155 K. So, at T_{str} parameters a and b are changed more than parameter c. All three parameter a, b, and c are reduced smoothly while decreasing the temperature further $T < 155$ K, however the c parameter behavior changes at T = 80 K. It starts to grow smoothly, and at 30 K it reaches its value, detected earlier at T_{str} (see Fig. 2(b)). The behavior of unit cell volume $V(T)$ also indicate the structural phase transition of the first order at $T_{str} = 155$ K. At further cooling down to 30 K the unit cell volume is reduced monotonically (see Fig. 2(c)).

Thus, while reducing the temperature from 295 K to $T_{str} = 155$ K crystal $GdFe_3(BO_3)_4$ is decreased (shorten) smoothly along the c

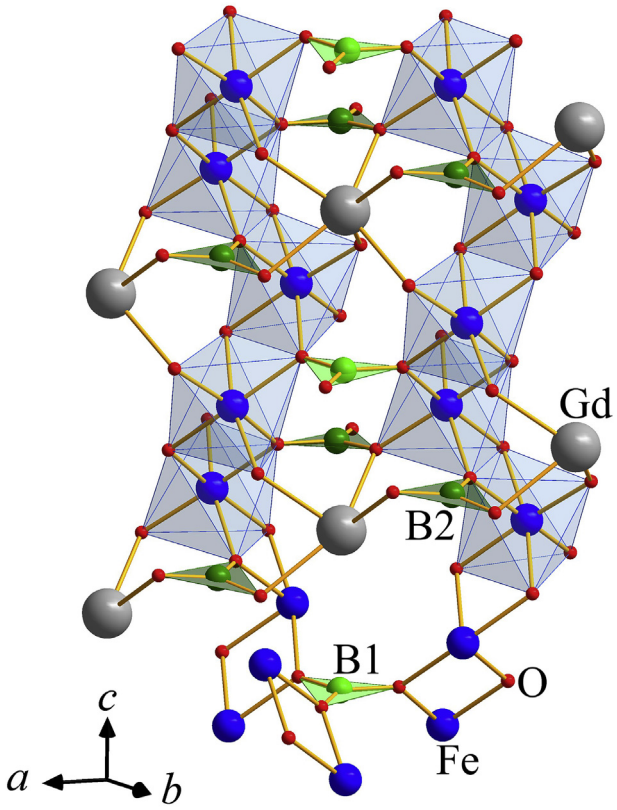

Fig. 1. Crystal structure of $GdFe_3(BO_3)_4$ at room temperature, T = 295 K. There are two types of boron triangles [BO_3] (B1 (light green balls) and B2 (green balls)), bonding Fe–Fe and Fe–Gd in planes (ab). (For interpretation of the references to colour in this figure legend, the reader is referred to the web version of this article.)

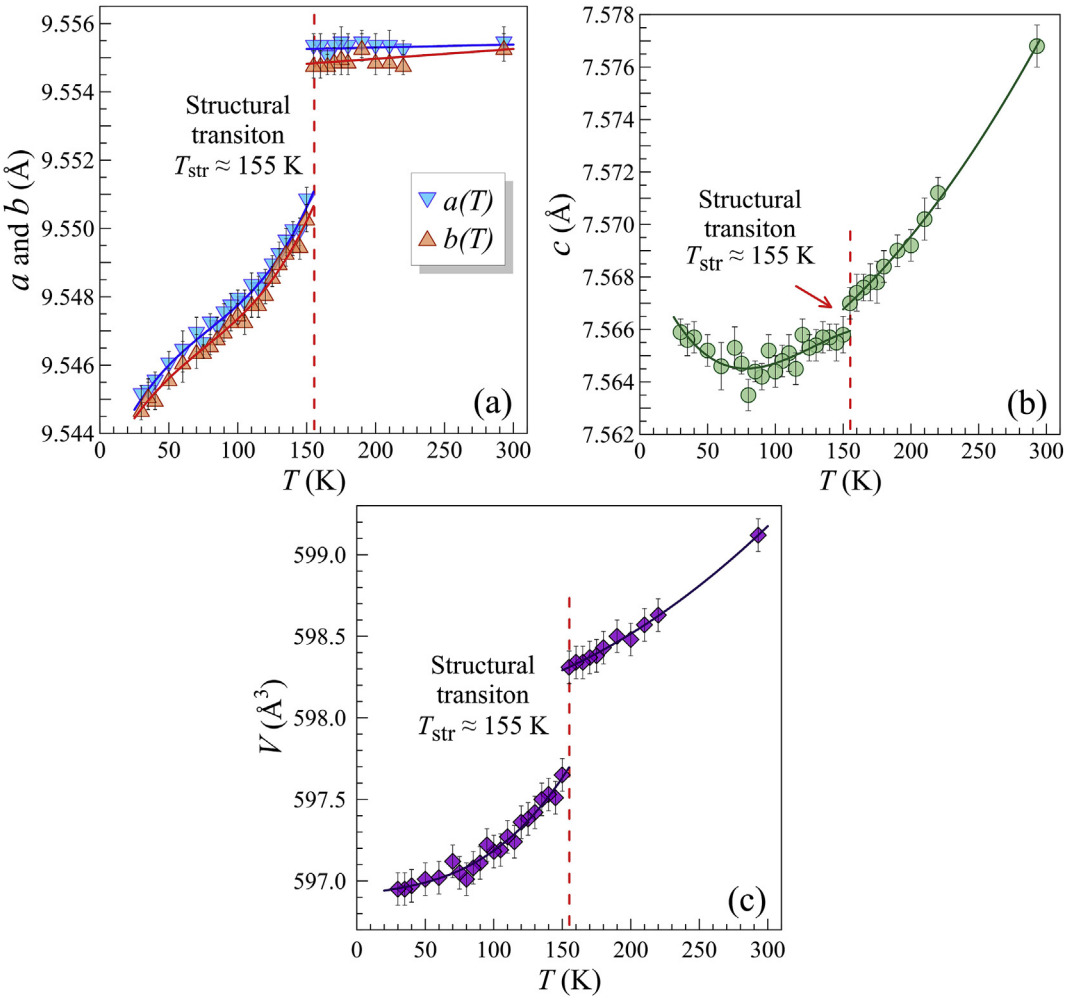

Fig. 2. Temperature dependences of the unit cell parameters of $GdFe_3(BO_3)_4$ crystal: *a* and *b* (a), *c* (b), and volume *V* (c). Solid lines are guides for the eye.

axis (by 0.01 Å), whereas the *a* and *b* axes remain unchanged. The sharp decrease in volume at T_{str} is mainly due to a reduction of the axes *a* and *b*, whereas the *c* axis at this point is reduced slightly. In the range of 155 – 80 K the crystal volume is reduced uniformly in all three axes. On further cooling from 80 to 30 K, the volume decreases only by reducing the parameters *a* and *b*, while the parameter *c* increases conversely. This effect is probably related to thermal expansion anomalies detected in a single crystal $GdFe_3(BO_3)_4$ in the range of $40 < T < 80$ K [16].

Note that in Refs. [26], the values of the parameters *a* and *b*, received at $T = 90$ K, are higher than at $T = 295$ K. Our structural experiments, by contrast, showed a reduction of the parameters *a* and *b* in the whole temperature range from 295 to 30 K. We have not found any structural features at the magnetic transition occurring at 38 K.

Taking into account the results obtained above the great interest is to conduct structural studies of $GdFe_3(BO_3)_4$ in a low-temperature region where magnetically ordered state is developed. Our group performed single-crystal structural analysis at 295, 90 and 30 K, and now the results are processed. Previously, our data support the change in the symmetry of the crystal from *R*32 to the $P3_121$ and the appearance of two non-equivalent structural positions of iron ions Fe1 and Fe2 below the structural transition at $T_{str} = 155$ K. The occupancy of iron ions with more symmetrical position Fe1 and common position Fe2 is in the ratio 1:2. Preliminary data indicate that when temperature is lowered from 90 to 30 K the oxygen octahedra surrounding ions Fe2 are distorted stronger than octahedra Fe1.

This distortion is mainly caused by change in distance between the iron ions and oxygen in the chains along the *c* axis. This correlates with the increase in the parameter *c* at 80 – 30 K (see Fig. 2(b)). At the same time the distance between the iron and oxygen bonding Fe with boron ions varies slightly. The distances Fe–Fe in the chains of both types (Fe1 and Fe2) and Fe–Gd distances increase. The full results of our single-crystal X-ray diffraction studies of $GdFe_3(BO_3)_4$ at 295, 90 and 30 K will be published in the near future.

3.2. Mössbauer spectroscopy

3.2.1. Paramagnetic temperature region structural phase transition at $T_S = 155$ K

In the temperature range 40 – 295 K Mössbauer spectra of $GdFe_3(BO_3)_4$ crystal have the form of a paramagnetic doublet with a small asymmetry of lines which width is in the range of 0.26 – 0.30 mm/s (see Fig. 3).

Taking into account our structural data pointing to two structural position of iron ions at $T < T_{str}$, in the first phase, we tried to approximate the Mössbauer spectra by two doublets with a variation of the isomer shifts δ and quadrupole splitting Δ. However, it

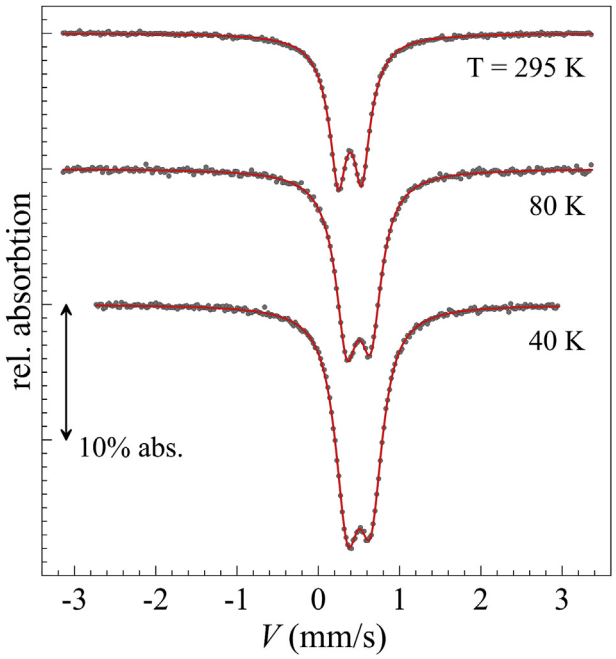

Fig. 3. Typical Mössbauer spectra of $GdFe_3(BO_3)_4$ crystal in paramagnetic temperature region.

was found that this model is unstable and gives a significant dispersion of hyperfine parameters of individual components. A detailed analysis of the different models of spectra processing at different temperatures in the range 40 – 295 K has demonstrated that one doublet approximation has highest stability of the parameters δ and Δ.

The temperature dependence of these parameters in the model of one doublet is shown in Fig. 4. The dependence $\delta(T)$ does not detect any anomalies in the region of 40 – 295 K, and its behavior is characteristic of the second-order Doppler effect. At 40 K the δ value is 0.504(5) mm/s and decreases to 0.390(5) mm/s at 295 K, which is typical for high-spin state of Fe^{3+} ions in octahedral oxygen coordination (see Table 1). The Δ value monotonically increases with temperature decreasing from 295 to 180 K, peaking near the temperature of the structural transition T_{str} = 155 K (see Fig. 4).

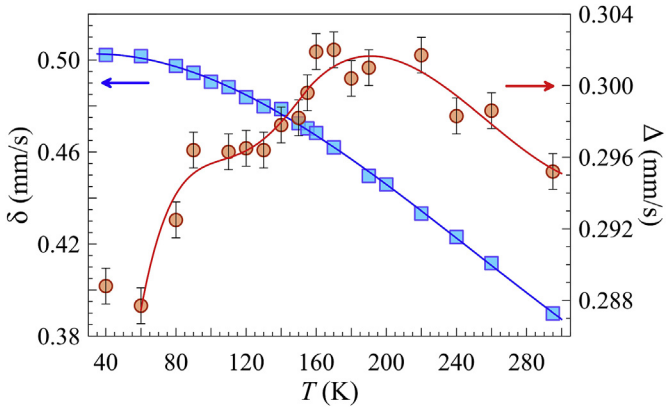

Fig. 4. Temperature dependences of the isomer shift δ (blue squares) and quadrupole splitting Δ (red circles). The uncertainties of isomer shift are within the squares. Solid lines are guides for the eye. (For interpretation of the references to colour in this figure legend, the reader is referred to the web version of this article.)

Upon further cooling to 130 K, the parameter Δ decreases rapidly to a value typical for room temperature, and then does not change while cooling down to 90 K. Below 90 K, the Δ again decreases dramatically. This region coincides with the temperature range where our structural studies reveal an anomaly in variations of the lattice parameter c (see Fig. 2(b)).

So, within some uncertainties the Mössbauer spectra (including the spectra of high statistics collected) do not indicate the existence of two structural position of iron ions in $GdFe_3(BO_3)_4$ expected at $T < T_{str} = 155$ K. In paramagnetic temperature region from 295 to 40 K the spectra are well characterized by single doublet until the magnetic phase transition at $T_N \approx 38$ K occurs. Evidently, the electronic states and local structure of iron ions in both Fe1 and Fe2 positions differ negligibly, and the parameters δ and Δ are equal in those positions. Nevertheless, the temperature behavior of the $\Delta(T)$ parameter correlates well with our structural data.

3.2.2. *Magnetic properties at $T < T_N = 38$ K*

When cooled below $T_N \approx 38$ K the Mössbauer spectra of $GdFe_3(BO_3)_4$ show the magnetic hyperfine splitting, indicating a magnetic phase transition. The best approximation of the low-temperature spectra is obtained by using three magnetic components (see Fig. 5), which differ in the value of the magnetic hyperfine field B_{hf} at iron nuclei and the value of the quadrupole shift. Two intensive sextet M1 (red) and M2 (blue) with close values of the hyperfine interaction parameters (see Table 1) correspond to two non-equivalent states of iron ions Fe1 and Fe2. The third low-intensity sextet M3 (green) presumably refers to the iron ions in contact with the impurity ions of bismuth, Bi, which partially replaced the gadolinium ions, Gd. Areas of the components M1 and M2 are in an approximate ratio 1:2. That is consistent with the X-ray diffraction data showed the distribution of the iron ions in two nonequivalent structural positions. Thus, the Mössbauer measurements results clearly allow to distinguish between the two iron ions states only when cooling system below the magnetic phase transition temperature $T_N = 38.0(1)$ K where strong magnetic interaction in the iron sublattice occurs.

According to our structural data, at 30 K (i.e. at $T < T_N$) there are changes of the Fe–O distances in the chains along the c axis, and the oxygen octahedra surrounding ions Fe2 are distorted stronger than octahedra around Fe1. The distances and bond angles Fe–O–Fe and Fe–O-Gd are changed simultaneously. One can assume that in addition to structural differences of octahedra Fe1 and Fe2 the nonequivalent magnetic state of iron M1 and M2 occur due to the interaction between the antiferromagnetic sublattices of iron and gadolinium.

Fig. 6 shows the temperature dependences of the magnetic hyperfine field B_{hf} at ^{57}Fe nuclei for three positions of the iron ions. To clarify the value of T_N and determine the type and dimensions of the magnetic ordering the experimental dependences $B_{hf}(T)$ near T_N were approximated by the calculated curves in the model of critical factors $B(T) = B_0(1-T/T_N)^{\beta}$.

In general, the magnetic behavior of the system can be characterized by the dimension of the magnetic lattice d and the dimension of an order parameter n. The parameter d can be 1 (one-dimensional chains), 2 (a layered structure or surface), and 3 (bulk material) (see, for example [30]). The parameter n is set by the model that describes the magnetic system, i.e., by Hamiltonian, H.

For $n = 1$ (Ising model): $H = -\Sigma J_{ij} S^2_i S^2_j$;
for $n = 2$ (planar model XY): $H = -\Sigma J_{ij}(S^a_i S^a_j + S^y_i S^y_j)$;
for $n = 3$ (Heisenberg model): $H = -\Sigma J_{ij} S_i S_j$.

For all n, a long-range order exists only for $d = 3$. Ising model ($n = 1$) allows two- and three-dimensional long-range order, and in

Table 1
Hyperfine parameters, obtained from Mössbauer spectra of $GdFe_3(BO_3)_4$ at certain temperatures.

	D		M1				M2				M3			
T (K)	Δ (mm/s)	Δ (mm/s)	δ (mm/s)	ε (mm/s)	B_{hf} (T)	A (%)	δ (mm/s)	ε (mm/s)	B_{hf} (T)	A (%)	δ (mm/s)	ε (mm/s)	B_{hf} (T)	A (%)
295	0.390(1)	0.295(1)	–	–	–	–	–	–	–	–	–	–	–	–
80	0.497(1)	0.293(1)	–	–	–	–	–	–	–	–	–	–	–	–
40	0.502(1)	0.289(1)	–	–	–	–	–	–	–	–	–	–	–	–
30	–	–	0.499(3)	0.112(6)	37.63(5)	27(1)	0.505(2)	0.087(3)	38.77(2)	58(1)	0.510(8)	0.12(2)	36.1(1)	15(1)
20	–	–	0.497(4)	0.084(8)	47.06(5)	28(1)	0.502(2)	0.086(3)	47.98(2)	62(1)	0.50(3)	−0.05(6)	45.0(5)	10(1)
5	–	–	0.505(1)	−0.222(2)	52.58(1)	30(1)	0.495(7)	−0.214(2)	53.29(1)	61(1)	0.488(5)	−0.213(9)	51.29(5)	9(1)

δ is the isomer shift, Δ is the quadrupole splitting, B_{hf} is the magnetic hyperfine field at Fe nuclei, ε is the quadrupole shift, A (%) is the relative area of the component.

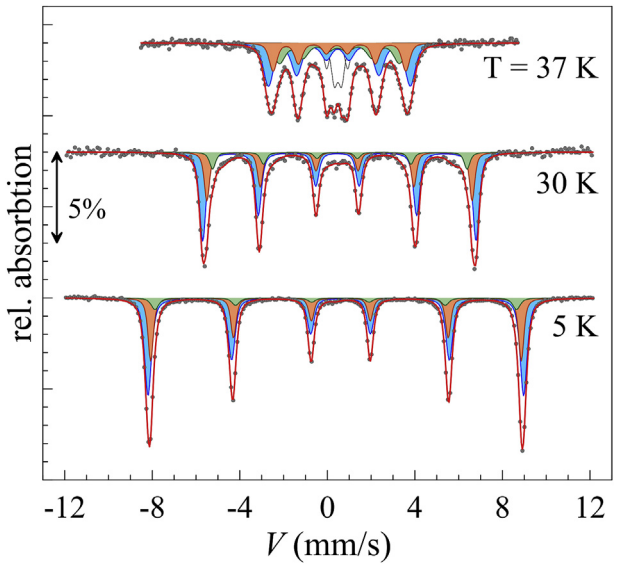

Fig. 5. Representative Mössbauer spectra of $GdFe_3(BO_3)_4$ crystal in magnetically ordered temperature region. There are M1 (red), M2 (blue), and M3 (green) components, corresponding to the nonequivalent magnetic state of iron. (For interpretation of the references to colour in this figure legend, the reader is referred to the web version of this article.)

Heisenberg model ($n = 1$) and XY ($n = 2$) a low-dimensional order ($d = 1$ and 2) does not exist. According to the model of critical coefficients a parameter β can take the following values [30,31]:

	$d = 3$			$d = 2$
n	1	2	3	1
β	0.31	0.33	0.35	0.125

For M1 component related to the helical chains of ions Fe1, we obtained the value $T_N = 38.0(1)$, and $\beta = 0.33(1)$ ($n = 2$), which corresponds to the two-dimensional Ising model. Structurally, all the atoms Fe1 are in exact positions on the axes of the third order, and there is no any partial disorder. Fe1 oxygen octahedra are distorted less than octahedra Fe2.

For M2 component related to helical chains ions Fe2, we obtained values $T_N = 38.0(1)$, and $\beta = 0.29(2)$ ($n = 1$). This corresponds to a one-dimensional Ising model. In terms of structure, the Fe2 atoms are arranged in less symmetrical common positions. The axis of the third order for them is lost, and there is structural disorder. Comparing with the paramagnetic region ($T = 90$ K) at $T < T_N$ the Fe2 oxygen octahedra are distorted more than octahedra Fe1, the Fe–Fe distance is increased by increasing the angle of the exchange coupling Fe–O–Fe. Apparently this is a reason for the fact that the magnetic hyperfine field B_{hf}(M2) for this component is slightly larger than for M1.

These data show that the quasi-one-dimensional ordering of the magnetic moments of iron take place in Fe2 chains, where the iron atoms are structurally disordered. Apparently this structural feature enhances the exchange interaction via oxygen along the chains Fe–O–Fe in the direction of the c axis. It has been suggested in Ref. [34] that as the temperature decreases, the 1D type of magnetic ordering is first to appear, because of the dominant role of antiferromagnetic exchange between adjacent layers. This leads to the magnetic ordering of helical iron chains along the c axis. Apparently, our data support this assumption.

For low-intensity M3 component, the values $T_N = 38.0(1)$ and $\beta = 0.37(1)$ ($n = 3$) are obtained, they correspond to the long-range magnetic order 3D. In the range of 15–29 K, the temperature dependence of the magnetic field $B_{hf}(T)$ for this component is markedly different from the curves for the components M1 and M2 (see Fig. 6). Apparently, this is due to the fact that the iron ions in the sublattice M3 are not influenced by gadolinium ions. Obviously, these iron ions have as a neighbor a bismuth ion instead of gadolinium ion. Bismuth is introduced as a gadolinium replacing

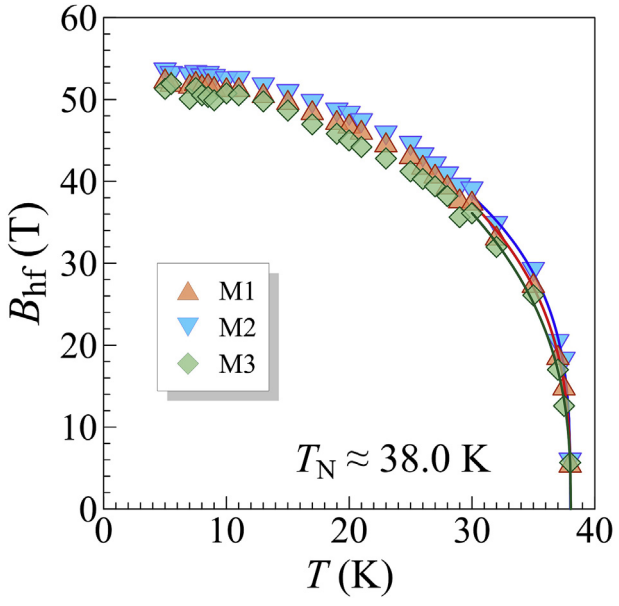

Fig. 6. Temperature dependences of the magnetic hyperfine field B_{hf} at ^{57}Fe nuclei in $GdFe_3(BO_3)_4$ crystal for different components of Mössbauer spectra. M1 – red triangles, M2 – blue inverse triangles, M3 – green diamonds. The uncertainties of the B_{hf} values are within the points. The solid differently colored lines are the calculated curves approximated to the critical coefficients model. (For interpretation of the references to colour in this figure legend, the reader is referred to the web version of this article.)

impurity in the process of the crystal growth.

The value of T_N found from our Mössbauer experiment, is slightly above the value of 37 K obtained by other methods [15,17,19]. This may be due to the fact that Mössbauer spectroscopy is more sensitive to magnetic correlations that can take place in the small temperature range above T_N, for example, in layered systems with competing exchange interactions [32].

3.2.3. Spin-reorientation phase transition (T_{SR} = 9 K)

Previously, using magnetic [19] and Mössbauer [22] measurements of the $GdFe_3(BO_3)_4$ crystal, spin reorientation phase transition in the subsystem of the iron ions has been discovered at temperatures of about 10 K. From the Mössbauer investigations of single crystals $GdFe_3(BO_3)_4$, we obtained values of the angle φ between the iron magnetic moments and the c axis at temperatures 5 and 20 K [22].

For the detailed study of the dynamics of reorientation transition, we conducted a thorough temperature scan of the Mössbauer spectra with interval of 0.5 − 1.0 K and obtained detailed dependence of the angle φ (T) in the range of 5 − 35 K.

It is known that the information about the orientation of the magnetic moment of iron ions can be obtained from the values of the quadrupole shift ε in Mössbauer spectra measured at temperatures below the magnetic ordering T_N. If the energy of the magnetic hyperfine interaction is much greater than the electric quadrupole one ($B_{hf} >> \Delta$), the observed quadrupole shift ε and the true value of the quadrupole splitting Δ (which can be obtained at temperatures above T_N) are related as:

$$\varepsilon = \Delta \frac{3\cos^2\varphi - 1}{2}$$

here φ is the angle between the magnetic moment of iron M and the main axis of the electric field gradient V_{zz}. Note, in $GdFe_3(BO_3)_4$ crystal, in view of the local C_3 symmetry, the V_{zz} direction coincides with the c axis [35]. Thus, the angular dependence $\varepsilon(\varphi)$ can be used to determine the direction of the magnetic moment of iron with respect to the crystallographic axes.

Fig. 7 shows the results of the calculation of the angle φ as determined from experimental Mössbauer spectra, which clearly shows the effect of spin reorientation. We have found that in the narrow temperature range 7 − 11 K, the φ tilt angle between the iron magnetic moments and the c axis sharply changes. In two iron sublattices Fe1 and Fe2, the φ angle value increases from 34° to ≈ 55° and to ≈ 63°, respectively. At higher temperatures, the $\varphi(T)$ dependences for both iron sublattices are almost linear. For ions Fe2, the angle goes to a "plateau" at $\varphi \approx 64°$ and remains mostly unchanged until the magnetic phase transition at $T \approx 35$ K. For ions Fe1 the value of φ increases monotonically from 55° to 68°. Fig. 8 shows a diagram of simulated reorientation of the iron magnetic moments in the Fe1 and Fe2 sites located in (ab) ferromagnetic plane relative to the crystallographic c axes at temperatures 5, 11, and 30 K.

It has been shown in Refs. [33,34] that below T_N = 38 K the gadolinium moments are polarized due to the antiferromagnetic interaction with iron, and the magnetic structure of $GdFe_3(BO_3)_4$ consists of the (ab) planes containing ferromagnetically ordered ions of iron and gadolinium. These planes alternate with translation along the c axis, and the neighboring planes are ordered antiferromagnetically. The magnetic properties are formed as a result of competition between anisotropic interactions of subsystems of iron and gadolinium ions with different signs of the anisotropy. In Refs. [36], the Neel temperature for Gd^{3+} ions of $T_N = 36.5(1)$ K has been found by the method of magnetic X-ray scattering.

With further cooling, the angle of Gd^{3+} moments to the c axis is

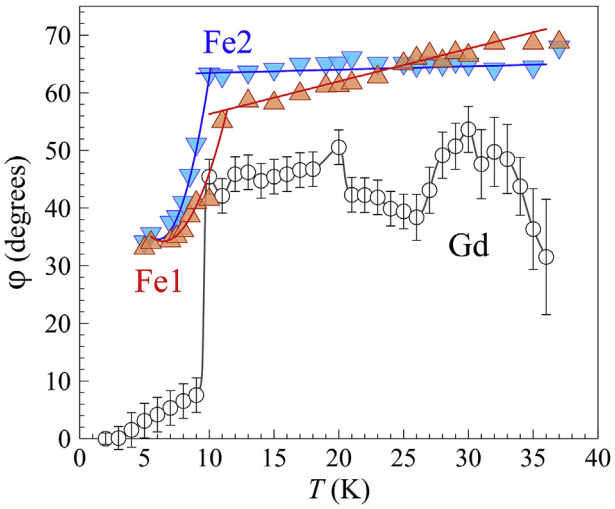

Fig. 7. Temperature dependences of angle φ between crystallographic axis c in $GdFe_3(BO_3)_4$ and magnetic moments of iron ions in two nonequivalent sites Fe2 (blue inverse triangles) and Fe1 (red triangles). Empty circles show the temperature dependence of φ for magnetic moments of Gd ions from data obtained in Ref. [36]. The uncertainties of the angles values are within the points. Solid lines are guides for the eye. (For interpretation of the references to colour in this figure legend, the reader is referred to the web version of this article.)

increased from 30° to about 60° at 30 K, and then reduced to 40° at 25 K. It remains almost the same (at about 45°) until the temperature of the spin reorientation phase transition that occurs at $T_{SR} \approx 9$ K simultaneously in both the iron and rare earth subsystems (see Figs. 7 and 8). According to our data, the temperature dependence of the angle φ (T) for the iron moments in the sublattices Fe1 and Fe2 in the range of 20–35 K is not correlated with the complex behavior of the orientation of gadolinium moments described in Refs. [36], as shown in Fig. 7. Below 20 K the magnetic moments of iron and gadolinium subsystems demonstrate consistent behavior terminating by the spin reorientation transition at T_{SR} = 10 K.

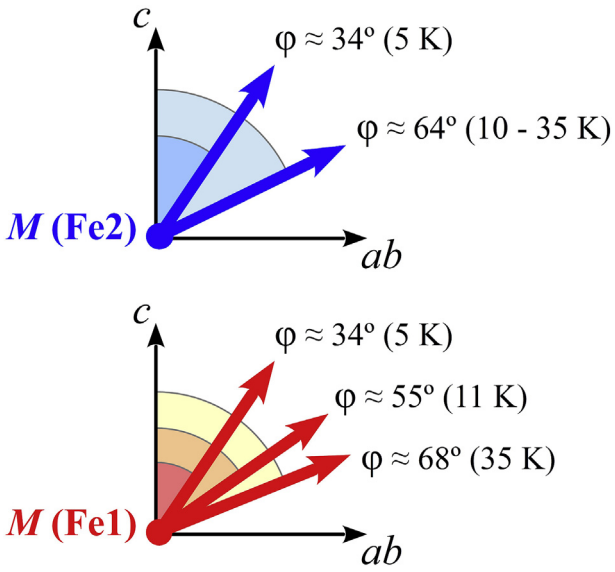

Fig. 8. The schema of reorientation of the iron magnetic moments in the Fe1 and Fe2 sites located in (ab) ferromagnetic plane based on the Mössbauer data obtained at T < 38 K.

In conclusion, we note that neutron studies of $GdFe_3(BO_3)_4$ have not been carried out because the Gd nuclei are not convenient for the neutron diffraction experiments. Therefore, assumptions about the type and dimensions of magnetic order as well as the dynamics of magnetic phase transitions have been made on the basis of measurements at external magnetic field, and theoretical calculations [33,34]. The results of the Mössbauer measurements obtained in this work have allowed for the first time to obtain the experimental data about the details of the magnetic transitions in $GdFe_3(BO_3)_4$.

Acknowledgments

We thank Dr. A.P. Dudka for help in the low temperature XRD measurements. This study was supported in part by the Russian Foundation for Basic Research (projects # 14-02-00483a and 13-02-12442), and the Council on Grants from the President of the Russian Federation for Support of Leading Scientific Schools (grant # NSh-1130.2014.5 and # NSh-924.2014.2). This work was performed using the equipment of the Shared Research Center IC RAS and was supported by the Russian Ministry of Education and Science (project RFMEFI62114X0005).

References

[1] J. Wang, J.B. Neaton, H. Zheng, V. Nagarajan, S.B. Ogale, B. Liu, D. Viehland, V. Vaithyanathan, D.G. Schlom, U.V. Waghmare, N.A. Spaldin, K.M. Rabe, M. Wuttig, R. Ramesh, Science 299 (2003) 1719.
[2] J. Li, J. Wang, M. Wuttig, R. Ramesh, N. Wang, B. Ruette, A.P. Pyatakov, A.K. Zvezdin, D. Viehland, Appl. Phys. Lett. 84 (2004) 5261.
[3] F. Bai, J. Wang, M. Wuttig, J.F. Li, N. Wang, A.P. Pyatakov, A.K. Zvezdin, L.E. Cross, D. Viehland, Appl. Phys. Lett. 86 (2005) 032511.
[4] T. Kimura, T. Goto, H. Shintani, K. Ishizaka, T. Arima, Y. Tokura, Nature 426 (2003) 55.
[5] T. Goto, T. Kimura, G. Lawes, A.P. Ramirez, Y. Tokura, Phys. Rev. Lett. 92 (2004) 257201.
[6] A.K. Zvezdin, S.S. Krotov, A.M. Kadomtseva, G.P. Vorob'ev, Yu F. Popov, A.P. Pyatakov, L.N. Bezmaternykh, E.A. Popova, JETP Lett. 81 (2005) 272.
[7] A.G. Zhdanov, A.K. Zvezdin, A.P. Pyatakov, T.B. Kosykh, D. Viehland, Phys. Solid State 48 (2006) 88.
[8] J.A. Campá, C. Cascales, E. Gutiérrez-Puebla, M.A. Monge, I. Rasines, C. Ruíz-Valero, Chem. Mater 9 (1997) 237.
[9] N.I. Leonyuk, L.I. Leonyuk, Progr. Cryst. Growth Charact. 31 (1995) 179.
[10] N.I. Leonyuk, Progr. Cryst. Growth Charact. 31 (1995) 279.
[11] D. Jaque, J. Alloys Compd. 323–324 (2001) 204.
[12] M. Huang, Y. Chen, X. Chen, Y. Huang, Z. Luo, Opt. Commun. 208 (2002) 163.
[13] X. Chen, Z. Luo, D. Jaque, J.J. Romero, J. Garcia Sole, Y. Huang, A. Jiang, C. Tu, J. Phys. Condens. Matter 13 (2001) 171.
[14] A.K. Zvezdin, G.P. Vorob'ev, A.M. Kadomtseva, YuF. Popov, A.P. Pyatakov, L.N. Bezmaternykh, A.V. Kuvardin, E.A. Popova, JETP Lett. 83 (2006) 509.
[15] M.N. Popova, J. Magn. Magn. Mater 321 (2009) 716.
[16] A.M. Kadomtseva, YuF. Popov, G.P. Vorob'ev, A.P. Pyatakov, S.S. Krotov, K.I. Kamilov, V.Yu Ivanov, A.A. Mukhin, A.K. Zvezdin, A.M. Kuz'menko, L.N. Bezmaternykh, I.A. Gudim, V.L. Temerov, Low. Temp. Phys. 36 (2010) 511.
[17] Y. Hinatsu, Y. Doi, K. Ito, K. Wakeshima, A. Alemi, J. Solid State Chem. 172 (2003) 438.
[18] A.D. Balaev, L.N. Bezmaternykh, I.A. Gudim, S.A. Kharlamova, S.G. Ovchinnikov, V.L. Temerov, J. Magn. Magn. Mater 258–259C (2003) 532.
[19] R.Z. Levitin, E.A. Popova, R.M. Chtsherbov, A.N. Vasiliev, M.N. Popova, E.P. Chukalina, S.A. Klimin, P.H.M. van Loosdrecht, D. Fausti, L.N. Bezmaternykh, JETP Lett. 79 (2004) 423.
[20] A.K. Zvezdin, V.M. Matveev, A.A. Mukhin, A.I. Popkov, Rare-earth Ions in the Magnetic Ordered Crystals, Nauka, Moscow, 1985.
[21] A.I. Pankrats, G.A. Petrakovski, L.N. Bezmaternykh, O.A. Bayukov, JETP 99 (2004) 766.
[22] S.A. Kharlamova, S.G. Ovchinnikov, A.D. Balaev, M.F. Thomas, I.S. Lyubutin, A.G. Gavriliuk, JETP 101 (2005) 1098.
[23] T. Kurumaji, K. Ohgushi, Y. Tokura, Phys. Rev. B 89 (2014) 195126.
[24] A.G. Gavriliuk, S.A. Kharlamova, I.S. Lyubutin, I.A. Troyan, S.G. Ovchinnikov, A.M. Potseluiko, M.I. Eremets, R. Boehler, JETP Lett. 80 (2004) 426.
[25] A.G. Gavriliuk, S.A. Kharlamova, I.S. Lyubutin, S.G. Ovchinnikov, A.M. Potseluyko, I.A. Trojan, V.N. Zabluda, J. Phys. Condens. Matter 17 (2005) 7599.
[26] S.A. Klimin, D. Fausti, A. Meetsma, L.N. Bezmaternykh, P.H.M. van Loosdrecht, T.T.M. Palstra, Acta Cryst. B 61 (2005) 481.
[27] D. Fausti, A.A. Nugroho, P.H.M. van Loosdrecht, S.A. Klimin, M.N. Popova, Phys. Rev. B 74 (2006) 024403.
[28] L.N. Bezmaternykh, S.A. Kharlamova, V.L. Temerov, Cryst. Rep. 49 (2004) 855.
[29] L.N. Bezmaternykh, V.L. Temerov, I.A. Gudim, N.A. Stolbovaya, Cryst. Rep. 50 (Suppl. 1) (2005) S97.
[30] L.J. De Jongh, in: L.J. De Jongh (Ed.), Magnetic Properties of Layered Transition Metal Compounds, Kluver Academic Publishers, Netherlands, 1990, p. 1.
[31] H.E. Stanley, Introduction to Phase Transitions and Critical Phenomena, Clarendon Press, Oxford, 1971, p. 42.
[32] H. Keller, I.M. Savic, Phys. Rev. B 28 (1983) 2638.
[33] A.I. Pankrats, G.A. Petrakovskii, L.N. Bezmaternykh, O.A. Bayukov, JETP 99 (2004) 476.
[34] A.M. Kadomtseva, YuF. Popov, S.S. Krotov, G.P. Vorob'ev, E.A. Popova, A.K. Zvezdin, L.N. Bezmaternykh, Low. Temp. Phys. 31 (2005) 807.
[35] N.N. Greenwood, T.C. Gibb, Mossbauer Spectroscopy, Chapman and Hall, London, 1978.
[36] H. Mo, C.S. Nelson, L.N. Bezmaternykh, V.T. Temerov, Phys. Rev. B 78 (2008) 214407.